


# Pharmacologic characterization of fluzoparib, a novel poly(ADP-ribose) polymerase inhibitor undergoing clinical trials

Lei Wang<sup>1</sup> | Changyong Yang<sup>2,3,4</sup> | Chengying Xie<sup>1</sup> | Jiahua Jiang<sup>2</sup> | Mingzhao Gao<sup>1</sup> | Li Fu<sup>1</sup> | Yun Li<sup>1</sup> | Xubin Bao<sup>1</sup> | Haoyu Fu<sup>1</sup> | Liguang Lou<sup>1</sup> 

<sup>1</sup>Shanghai Institute of Materia Medica, Chinese Academy of Sciences, Shanghai, China

<sup>2</sup>Jiangsu Hengrui Medicine Co Ltd, Lianyungang, China

<sup>3</sup>Pharmaceutical Research Center and School of Chemistry and Chemical Engineering, Southeast University, Nanjing, China

<sup>4</sup>Jiangsu Province Hi-Tech Key Laboratory for Biomedical Research, Southeast University, Nanjing, China

## Correspondence

Liguang Lou, Shanghai Institute of Materia Medica, Chinese Academy of Sciences, Shanghai, China.

Email: lg lou@mail.shcnc.ac.cn

## Funding information

National Natural Science Foundation of China, Grant/Award Number 81502636; Yunnan Provincial Science and Technology Department, Grant/Award Number 2017ZF010; Science and Technology Commission of Shanghai Municipality, Grant/Award Number 14DZ2294100

Poly(ADP-ribose) polymerase (PARP) enzymes play an important role in repairing DNA damage and maintaining genomic stability. Olaparib, the first-in-class PARP inhibitor, has shown remarkable clinical benefits in the treatment of *BRCA*-mutated ovarian or breast cancer. However, the undesirable hematological toxicity and pharmacokinetic properties of olaparib limit its clinical application. Here, we report the first preclinical characterization of fluzoparib (code name: SHR-3162), a novel, potent, and orally available inhibitor of PARP. Fluzoparib potently inhibited PARP1 enzyme activity and induced DNA double-strand breaks, G<sub>2</sub>/M arrest, and apoptosis in homologous recombination repair (HR)-deficient cells. Fluzoparib preferentially inhibited the proliferation of HR-deficient cells and sensitized both HR-deficient and HR-proficient cells to cytotoxic drugs. Notably, fluzoparib showed good pharmacokinetic properties, favorable toxicity profile, and superior antitumor activity in HR-deficient xenografts models. Furthermore, fluzoparib in combination with apatinib or with apatinib plus paclitaxel elicited significantly improved antitumor responses without extra toxicity. Based on these findings, studies to evaluate the efficacy and safety of fluzoparib (phase II) and those two combinations (phase I) have been initiated. Taken together, our results implicate fluzoparib as a novel attractive PARP inhibitor.

## KEYWORDS

antitumor activity, fluzoparib, pharmacokinetics, poly(ADP-ribose) polymerase, toxicity

## 1 | INTRODUCTION

The family of PARPs is characterized by the ability to catalyze the addition of PAR to their target proteins.<sup>1</sup> Poly (ADP-ribose) polymerase 1, which accounts for 80% of cellular PARP activity, functions as a DNA repair factor in various DNA repairing processes.<sup>1</sup> Mechanically, PARP1 is recruited to DNA damage sites and catalyzes PAR synthesis, leading to increased redistribution of PARP1

on activated genes, modulation of the chromatin structure, and recruitment of the DNA repair machinery.<sup>2</sup> In addition, PARP1 plays a role in cellular processes such as transcriptional regulation, telomere cohesion, and mitotic spindle formation.<sup>3</sup>

Poly(ADP-ribose) polymerase inhibitors show effective single-agent activity against cancers harboring HR defects. *BRCA1/2* defects are the most extensively studied indication involved in HR in regards to PARP inhibition. A cell that is *BRCA*-deficient has reduced

**Abbreviations:** CDK, cyclin-dependent kinase; DSB, DNA double-strand break; HR, homologous recombination repair; PAR, polymer of ADP-ribose; PARP, poly(ADP-ribose) polymerase; PDX, patient-derived xenograft; TGI, tumor growth inhibition; TMZ, temozolomide.

This is an open access article under the terms of the Creative Commons Attribution-NonCommercial License, which permits use, distribution and reproduction in any medium, provided the original work is properly cited and is not used for commercial purposes.

© 2019 The Authors. *Cancer Science* published by John Wiley & Sons Australia, Ltd on behalf of Japanese Cancer Association.

capacity to repair DNA DSBs by HR and is consequently hypersensitive to PARP inhibitors through the concept of synthetic lethality.<sup>4,5</sup> The finding that PARP inhibition is exquisitely effective against BRCA-deficient cancers greatly boosts the development of PARP inhibitors as anticancer agents.<sup>6</sup> Olaparib was the first PARP inhibitor to be introduced into the clinic for the treatment of BRCA-mutated ovarian cancer and is the first and only PARP inhibitor approved in BRCA-mutated, HER2-negative metastatic breast cancer. To date, 3 PARP inhibitors (olaparib, rucaparib, and niraparib) have been approved by the FDA.

Responses to PARP inhibitors among patients with BRCA-mutated ovarian or breast cancer are sufficiently profound to support the approval of these agents, but treatment-related toxicities are common and restrict the clinical applications of PARP inhibitors.<sup>7</sup> Among the three approved PARP inhibitors, niraparib has the highest rate of thrombocytopenia; 14.7% of patients discontinued treatment due to toxicity and 68.9% required dose reductions in the ENGOT-OV16/NOVA trial.<sup>8</sup> Rucaparib has the highest rate of elevations in liver transaminases and 55% of patients required dose reductions in the ARIEL3 trial.<sup>9</sup> Olaparib shows a relatively safe profile: apart from anemia, toxicities related to olaparib were low grade.<sup>10</sup> Nonetheless, the toxicity remains an issue of concern and 25% of patients required dose reductions in the SOLO2/ENGOT-Ov21 trial.<sup>11</sup> One of the major obstacles restricting the safety and efficacy of olaparib is its undesirable pharmacokinetic properties. Olaparib has a short half-life and the exposure of olaparib achieved in tumor is only approximately 40% of that in plasma.<sup>12</sup> In the clinic, patients need to take 8 capsules twice a day (400 mg per dose) or 2 tablets twice a day (300 mg per dose) to ensure the efficacy of the drug. Because of individual variations in drug metabolism, the high dosage of olaparib leads to high coefficient of variation of drug exposure and concentrations,<sup>10</sup> which results in severe toxicity in some patients. Therefore, further structural modification and optimization of olaparib to improve the pharmaceutical properties and toxicity profile is of significant clinical value.

In order to improve the efficacy and expand the indications of PARP inhibitors, great efforts have been made to explore the combination of PARP inhibitors with other therapeutic agents, such as alkylating agents (temozolomide), platinum agents, and taxanes.<sup>13</sup> However, in clinical trials, PARP inhibitors combined with temozolomide led to severe hematological toxicity,<sup>14</sup> and PARP inhibitors combined with paclitaxel had no significant improvement in the overall survival.<sup>15</sup> Therefore, more efforts are needed to explore optimal combination regimens.

We rationally designed and synthesized a series of derivatives based on the chemical structure of olaparib. One derivative, fluzoparib (code name: SHR-3162), stood out in the screening and was selected for further evaluation. Fluzoparib was comparable to olaparib in various models in vitro and superior to olaparib in vivo. Notably, fluzoparib showed favorable drug-like properties. We further explored several combination regimens and found that a 2-drug combination of fluzoparib with apatinib and a 3-drug combination including fluzoparib, paclitaxel, and

apatinib elicited remarkable antitumor responses without extra toxicity. Because of the impressive preclinical activity of fluzoparib, clinical trials have been initiated in China (NCT02575651, NCT03026881, NCT03062982, NCT03075462, NCT03509636, and NCT03645200). Here, we present the first report of the major preclinical pharmacological results of fluzoparib.

## 2 | MATERIALS AND METHODS

### 2.1 | Reagents and Abs

Fluzoparib was provided by Jiangsu Hengrui Medicine Co. (Shanghai, China). Olaparib was purchased from Selleckchem (Houston, TX, USA). Antibodies against  $\gamma$ H2AX, p-CDK1, cyclin B1, caspase 8, caspase 9, cleaved caspase 3, and  $\beta$ -tubulin were purchased from Cell Signaling Technology (Beverly, MA, USA). Anti-RAD51 antibody was purchased from Santa Cruz Biotechnology (Santa Cruz, CA, USA). Anti-PAR Ab and PARP universal colorimetric assay kit were purchased from Trevigen (Gaithersburg, MD, USA).

### 2.2 | Cell culture

V-C8 and V-C8#13-5 cell lines were kindly provided by Professor M. Zdzienicka (Leiden University, Amsterdam, the Netherlands). UWB1.289, UWB1.289+BRCA1, MDA-MB-436, MX-1, SW620, and NCI-N87 cell lines were purchased from ATCC (Manassas, VA, USA). The OVCAR-8 cell line was purchased from the NCI-Frederick Cancer DCTD Tumor Repository (Frederick, MD, USA). Cells were cultured according to instructions provided by the manufacturers.

### 2.3 | Enzyme activity

The inhibition on PARP1 enzymatic activity was determined by ELISA according to the manufacturer's instructions.  $A_{450}$  was measured using Synergy H4 Hybrid Microplate Reader (BioTek Instruments, Winooski, VT, USA). The inhibition rate was calculated as  $(A_{450\text{control}} - A_{450\text{treated}} / A_{450\text{control}}) \times 100\%$ . Half maximal inhibitory concentration ( $IC_{50}$ ) was determined with GraphPad Prism software (GraphPad Software Inc., La Jolla, CA, USA).

### 2.4 | Molecular docking

The PARP1 structure from a crystal of PARP1/olaparib complex<sup>16</sup> was used as the template structure. The X-ray crystal structure of this PARP1/olaparib complex was obtained from the Protein Data Bank (PDB code: 5DS3). Glide, LigPrep, Maestro and PyMOL were obtained from Schrödinger (New York, NY, USA). Molecular docking was carried out using Glide version 6.9 in its SP mode. LigPrep version 3.6 was applied to preprocess the compound using default parameters. The obtained docked poses were analyzed with Maestro, PyMOL, and LigPlot (European Bioinformatics Institute, Hinxton, Cambridgeshire, UK).

## 2.5 | Cell proliferation assay

Cells were treated with PARP inhibitors alone or in combination with the indicated anticancer drugs for 3 days (V-C8, V-C8#13-5, UWB1.289, and UWB1.289+BRCA1) or 5 days (all the other cells). The  $IC_{50}$  values were determined by sulforhodamine B assay as described previously.<sup>17</sup>

## 2.6 | Western blot analysis

The standard western blotting<sup>17</sup> was used to detect the changes in protein levels caused by the indicated treatments.

## 2.7 | Cell cycle analysis

Cells were fixed in ethanol and stained with propidium iodide following standard methods. The cell cycle was analyzed by FACS using a FACScan flow cytometer (BD Biosciences, San Jose, CA, USA).

## 2.8 | Animal studies

### 2.8.1 | Pharmacokinetic/pharmacodynamic studies in mice

Female Balb/cA nude mice (5-6 weeks old) were purchased from Shanghai Laboratory Animal Center, Chinese Academy of Sciences (Shanghai, China). Studies were carried out as described previously.<sup>16</sup> Briefly, mice bearing MDA-MB-436 tumors received a single p.o. dose of fluzoparib (0.3, 1, or 3 mg/kg) and then tumor tissue and blood were collected at multiple time points (0, 2, 4, 8, 12, and 24 hours) post-dosing. Concentrations of fluzoparib in plasma and tumor were determined by HPLC/tandem mass spectrometry. Tumor samples were lysed with RIPA buffer and analyzed by western blotting.

### 2.8.2 | Pharmacokinetic studies in rats

Female SD rats received a single oral dose of fluzoparib (4 mg/kg) and then blood was collected at multiple time points (0, 0.25, 0.5, 0.75, 1, 1.5, 2, 4, 8, 12, and 24 hours) post-dosing. Concentrations of fluzoparib in plasma were determined by HPLC/tandem mass spectrometry.

To determine bioavailability, female SD rats were injected i.v. with fluzoparib (4 mg/kg) and then blood was collected at multiple time points (0, 0.08, 0.25, 0.5, 1, 1.5, 2, 4, 6, 8, 12, and 24 hours) post-dosing. Concentrations of fluzoparib in plasma were determined by HPLC/tandem mass spectrometry.

### 2.8.3 | Acute toxicity in mice

Mice (female,  $n = 6$ ) received a single oral dose of fluzoparib at 1000 mg/kg. Individual body weight was measured for 21 days.

### 2.8.4 | Acute and chronic toxicity in rats

In the acute toxicity study, SD rats (female,  $n = 6$ ) received a single oral dose of fluzoparib at 2000 mg/kg and were observed for 14 days. In the chronic toxicity study, SD rats (female,  $n = 15$ ) received fluzoparib at 30 mg/kg for the first 66 days, at 60 mg/kg for the next 24 days, and were then observed for another 28 days without treatment. Clinical signs and histopathology were examined in both studies.

### 2.8.5 | Cell-line-derived xenograft model

Tumor models were established by s.c. inoculating female nude mice with MDA-MB-436 or MX-1 cells. When tumors reached a volume of 100-300 mm<sup>3</sup>, mice were randomized into control ( $n = 10-12$ ) or treatment ( $n = 6$ ) groups. Control group was given vehicle alone, and treatment groups received fluzoparib (p.o.), olaparib (p.o.), and temozolomide (p.o.) alone or in combination.

### 2.8.6 | Patient-derived xenograft model

Animal studies using gastric model STO#069 were carried out by GenenDesign (Shanghai, China). Tumor fragments with the volume of 15-30 mm<sup>3</sup> were s.c. implanted into right flanks of Balb/c nude mice. When tumor sizes reached 150-250 mm<sup>3</sup>, mice were randomly divided into control ( $n = 6$ ) or treatment ( $n = 6$ ) groups. Control group was given vehicle (p.o.) and treatment groups were given fluzoparib (p.o.), apatinib (p.o.), cisplatin (i.p.), and paclitaxel (i.p.) alone or in combination.

Tumor volume was calculated as  $(\text{length} \times \text{width}^2)/2$ , and body weight was monitored as an indicator of general health. Tumor growth inhibition (TGI) (%) was calculated as  $100 - (T_t - T_0)/(C_t - C_0) \times 100$ . When  $T_t < T_0$  or  $C_t < C_0$ , TGI (%) was calculated as  $100 - (T_t - T_0)/T_0 \times 100$ .  $T_t$  = mean tumor volume of treated at time  $t$ ,  $T_0$  = mean tumor volume of treated at time 0,  $C_t$  = mean tumor volume of control at time  $t$  and  $C_0$  = mean tumor volume of control at time 0.

All animal experiments were carried out in accordance with guidelines of the Institutional Animal Care and Use Committee at the Shanghai Institute of Materia Medica, Chinese Academy of Sciences.

## 2.9 | Statistical analysis

Data were analyzed with GraphPad Prism software. Two-tailed Student's  $t$  tests were used to determine the statistical significance of differences between 2 groups.

## 3 | RESULTS

### 3.1 | Fluzoparib is a potent inhibitor of PARP1

We first examined the inhibitory activities of fluzoparib (Figure 1A) in a cell-free enzymatic assay against PARP1. Fluzoparib significantly

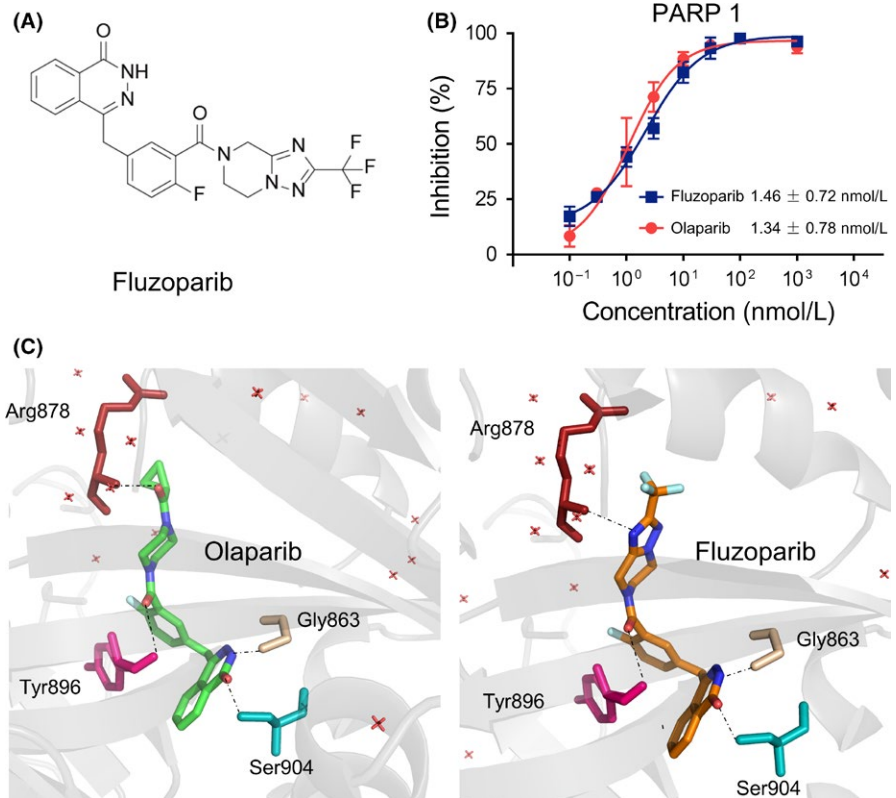


**FIGURE 1** Characterization of fluzoparib as a poly(ADP-ribose) polymerase (PARP) inhibitor. A, Chemical structure of fluzoparib. B, PARP inhibition measured by ELISA. Error bars represent mean ± SD. C, Molecular modeling of the PARP1-olaparib/fluzoparib complex. Key residues of PARP1 were shown as sticks. Hydrogen bonds are shown as dashed lines

inhibited PARP1 activity, with an IC<sub>50</sub> value of 1.46 ± 0.72 nmol/L, which was close to that of olaparib (IC<sub>50</sub>, 1.34 ± 0.78 nmol/L) (Figure 1B). We then explored the binding sites of fluzoparib in PARP1 using structural modeling. As shown in Figure 1C, fluzoparib was well ordered in the catalytic active site of PARP1 with the same binding mode as olaparib. Together, these data indicate that fluzoparib is a potent PARP1 inhibitor.

### 3.2 | Fluzoparib induces persistent DSBs in HR-deficient cells

Unrepaired single-strand breaks induced by PARP1 inhibition will eventually be converted to DSBs, which can be normally repaired by HR.<sup>18</sup> We detected RAD51 foci, the indicator of HR repair, after treatment with PARP1 inhibitors (Figure 2A). Fluzoparib induced the formation of RAD51 foci in V-C8#13-5 cells, indicating that DSBs were induced by drug treatment and HR function was proficient in the cells. In contrast, fluzoparib did not induce RAD51 foci in V-C8 cells, confirming the deficiency of HR function (*BRCA2*-deficient) in the cells. We next detected DSB accumulation using  $\gamma$ H2AX as a marker. Fluzoparib increased the levels of  $\gamma$ H2AX in a concentration-dependent manner in both *BRCA2*-deficient V-C8 cells and *BRCA1*-deficient MDA-MB-436 cells, but not in *BRCA*-proficient V-C8#13-5 cells (Figure 2B), indicating that DSBs were induced and persistent in HR-deficient cells. The DSB-inducing capacity of fluzoparib was similar to that of olaparib. Together, these results suggest that, following treatment with fluzoparib, DSBs are induced in both HR-proficient and HR-deficient cells, but only persistent in HR-deficient cells.

### 3.3 | Fluzoparib induces G<sub>2</sub>/M arrest and apoptosis in HR-deficient cells

DNA DSBs are supposed to evoke the G<sub>2</sub>/M checkpoint in cells, leading to G<sub>2</sub>/M phase arrest and eventual apoptosis.<sup>19</sup> We thus checked CDK1 and cyclin B, the key regulators of G<sub>2</sub>-phase transition, after treatment with fluzoparib in MDA-MB-436 cells (*BRCA1*-deficient). As shown in Figure 2C, fluzoparib increased levels of both pCDK1 and cyclin B, indicating activation of the G<sub>2</sub>/M checkpoint. We then determined the cell cycle profile in these cells. Consistently, fluzoparib induced G<sub>2</sub>/M phase arrest in a concentration-dependent manner (Figure 2D). We further assessed apoptosis after long-term treatment with fluzoparib by determining the intermediate cleavage products of crucial apoptosis mediators. Fluzoparib concentration-dependently increased the processing of caspase-3, -8, and -9, indicating that apoptosis was induced through both mitochondrial and death receptor pathways (Figure 2E). Together, these data suggest that fluzoparib induces G<sub>2</sub>/M arrest and apoptosis in HR-deficient cells.

### 3.4 | Fluzoparib selectively inhibits proliferation of HR-deficient cancer cells and sensitizes both HR-deficient and HR-proficient cancer cells to cytotoxic drugs

We next evaluated the antiproliferative effects of fluzoparib among a panel of cell lines with distinct genotypes. Fluzoparib was preferentially efficacious against HR-deficient cells, such as *BRCA1*-deficient

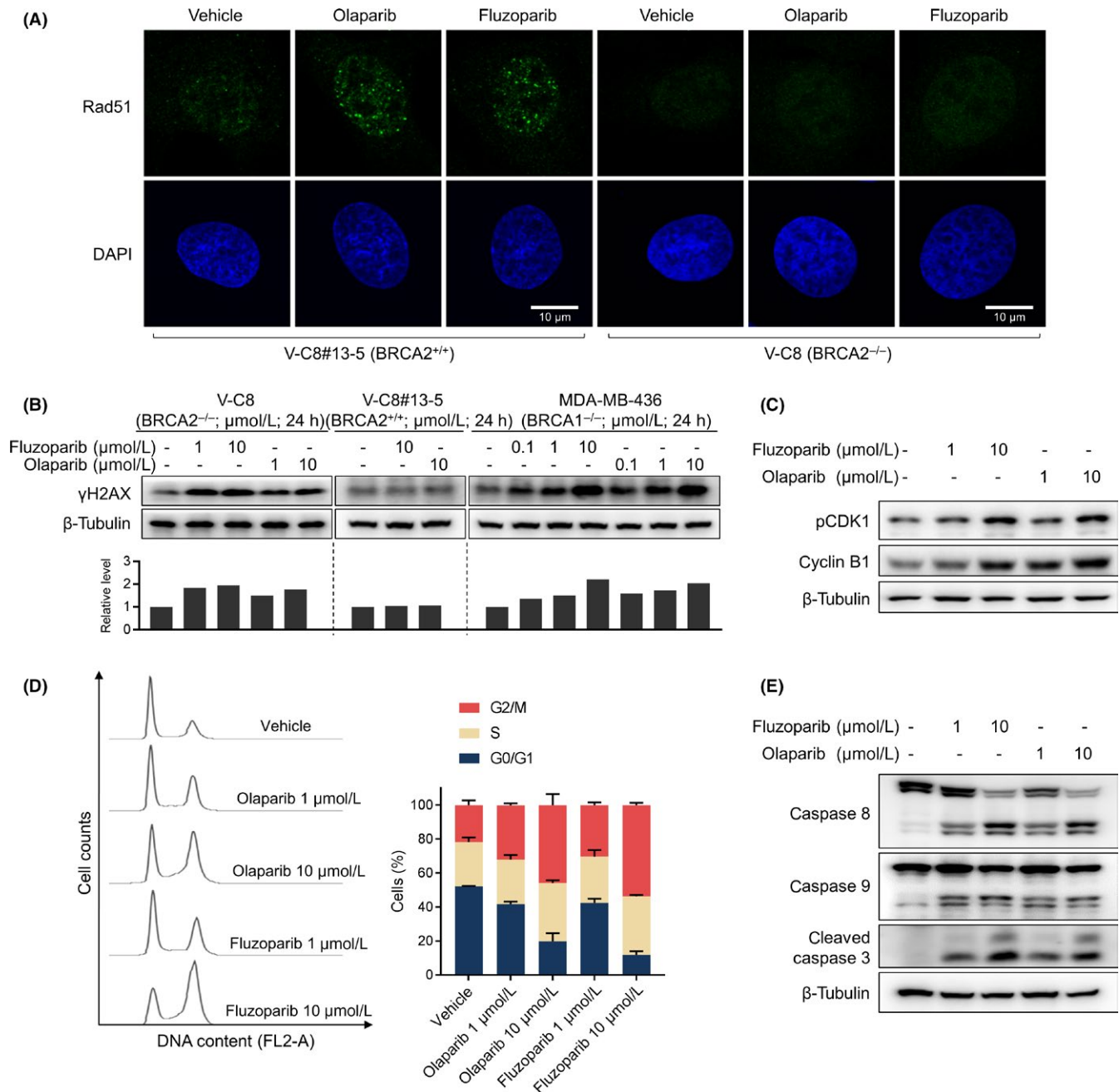


**FIGURE 2** Double-strand break induction, G<sub>2</sub>/M arrest, and apoptosis in homologous recombination repair-deficient cells. A, V-C8 and V-C8#13-5 cells were treated with fluzoparib (30 μmol/L) or olaparib (30 μmol/L) for 24 hours. Rad51 was detected by immunofluorescence. Scale bar = 10 μm. B, V-C8, V-C8#13-5, and MDA-MB-436 cells were treated with fluzoparib or olaparib for 24 hours. γH2AX accumulation was detected by western blotting and quantified by densitometry. C, MDA-MB-436 cells were treated with fluzoparib or olaparib for 24 hours. p-CDK1 and cyclin B1 were detected by western blotting. D, MDA-MB-436 cells were treated with fluzoparib or olaparib for 48 hours. Cell cycle was analyzed by flow cytometry. Left, representative images; Right, data from 3 separate experiments expressed as mean ± SD. E, MDA-MB-436 cells were treated with fluzoparib or olaparib for 72 hours. Whole cell lysates were detected by western blotting

(UWB1.289 and MDA-MB-436), BRCA2-deficient (V-C8), BRCA1-deficient/BRCA2-mutated (MX-1), and BRCA1 hypermethylated (OVCAR-8) cells, but not HR-proficient (V-C8#13-5 and UWB1.289 BRCA1) cells (Table 1). Fluzoparib showed similar antiproliferative effects to olaparib in all these cells.

The combination of PARP inhibitor with cytotoxic drugs is a rational strategy in the clinic. We thus evaluated the antiproliferative effects of fluzoparib combined with TMZ, cisplatin, or paclitaxel. As shown in Figure 3, the extent of synergy achieved by the fluzoparib/TMZ combination is maximal in comparison with the other

**TABLE 1** Antiproliferative activity of fluzoparib against cells with distinct genotypes

Cell line	Type	HR function	IC <sub>50</sub> (μmol/L, mean ± SD)	
			Fluzoparib	Olaparib
V-C8	Chinese hamster lung fibroblasts	BRCA2 <sup>-/-</sup>	0.053 ± 0.038	0.035 ± 0.020
V-C8 #13-5	Chinese hamster lung fibroblasts	BRCA2 <sup>+/+</sup>	>10	>10
UWB1.289	Ovarian cancer	BRCA1 <sup>-/-</sup>	0.51 ± 0.22	0.36 ± 0.24
UWB1.289+BRCA1	Ovarian cancer	BRCA1 <sup>+/+</sup>	>10	>10
MDA-MB-436	Breast cancer	BRCA1 <sup>-/-</sup>	1.57 ± 0.16	1.23 ± 0.15
MX-1	Breast cancer	BRCA1 <sup>-/-</sup> , BRCA2 mutated	1.57 ± 0.43	1.43 ± 0.26
OVCAR-8	Ovarian cancer	BRCA1 hypermethylation	1.43 ± 0.20	2.16 ± 0.50

Cells were treated with different concentrations of drugs and cell proliferation was measured using sulforhodamine B assays. Data shown represent mean ± SD of 3 independent experiments. HR, homologous recombination repair

combinations. Fluzoparib significantly potentiated the cytotoxicity of TMZ in both HR-deficient and HR-proficient cancer cells with an average potentiation index of 54.2 (range, 4.9–187.5). Fluzoparib showed relatively weak sensitization to cisplatin and paclitaxel, with an average potentiation index of 13.7 (range, 5.1–23.1) and 2.7 (range, 1.2–3.8), respectively.

Collectively, the data suggest that fluzoparib is a PARP inhibitor with potent in vitro anticancer activity.

### 3.5 | Pharmacokinetic/pharmacodynamic characteristics of fluzoparib

We then assessed the pharmacokinetic profile of fluzoparib in MDA-MB-436 xenograft-bearing mice. After a single oral dose at 0.3, 1, or 3 mg/kg, fluzoparib was rapidly absorbed and rapidly cleared from blood at all dose levels; plasma concentrations of fluzoparib quickly reached maximum within 2 hours and were merely detected (<1.0 ng/mL) at 24 hours post dosing (Figure 4A). In contrast, concentrations of fluzoparib in tumor remained at high levels even at 24 hours after dosing (57.9 ± 16.6, 39.3 ± 8.2, and 85.6 ± 102.0 ng/g for doses of 0.3, 1, and 3 mg/kg, respectively). The exposure of fluzoparib increased over its dose escalation in both plasma and tumor. Notably, the exposure (AUC<sub>0-24 hours</sub>) of fluzoparib in tumor was 25.0, 14.6, and 6.7-fold higher than that in plasma for doses 0.3, 1, and 3 mg/kg, respectively. We further assessed the pharmacokinetic profile of fluzoparib in female rats. After a single oral dose at 4 mg/kg, the exposure (AUC<sub>0-24 hours</sub>) of fluzoparib was 3293.1 μg-hour/L, which was higher than that of olaparib reported at 5 mg/kg (2380 μg-hour/L).<sup>20</sup> Moreover, the bioavailability of fluzoparib (35.8%) was also higher than that of olaparib (<20%).<sup>20</sup>

We next evaluated the effects of fluzoparib on the formation of PAR, a pharmacodynamic marker reflecting the suppression

of PARP,<sup>10</sup> in MDA-MB-436 xenograft-bearing mice. Fluzoparib showed a strong inhibition on PAR formation in a dose- and time-dependent manner (Figure 4B). Fluzoparib at 0.3 mg/kg did not affect PAR formation, at 1 mg/kg significantly reduced PAR formation, and at 3 mg/kg resulted in almost complete disappearance of the PAR formation.

Collectively, these results suggest that fluzoparib possesses favorable pharmacokinetic characteristics and can inhibit PARP in vivo.

### 3.6 | Acute and chronic toxicity of fluzoparib

The acute toxicity of fluzoparib was investigated in both mice and rats. A single oral dose of fluzoparib at either 1000 mg/kg in female mice or 2000 mg/kg in female rats caused no mortalities or adverse signs. All mice (Figure 5A) and rats (Figure 5B) gained weight over the course of the study. The chronic toxicity of fluzoparib was also investigated. Female rats received daily oral treatment with fluzoparib at 30 mg/kg for the first 66 days, at 60 mg/kg for the following 24 days, and then were observed for another 28 days without treatment. There were no abnormal changes in clinical signs or body weights (Figure 5C) during the study. Thus, fluzoparib is a drug with a good toxicity profile.

### 3.7 | In vivo antitumor activity of fluzoparib in cancer cell-line-derived xenograft models

The antitumor potential of fluzoparib was investigated in MDA-MB-436 (BRCA1-deficient) xenograft models in vivo. As shown in Figure 6A, fluzoparib apparently inhibited the growth of tumor with an inhibition rate of 59% (day 21) at 30 mg/kg, and olaparib led to an inhibition rate of 44% (day 21) at the same dosage. Neither

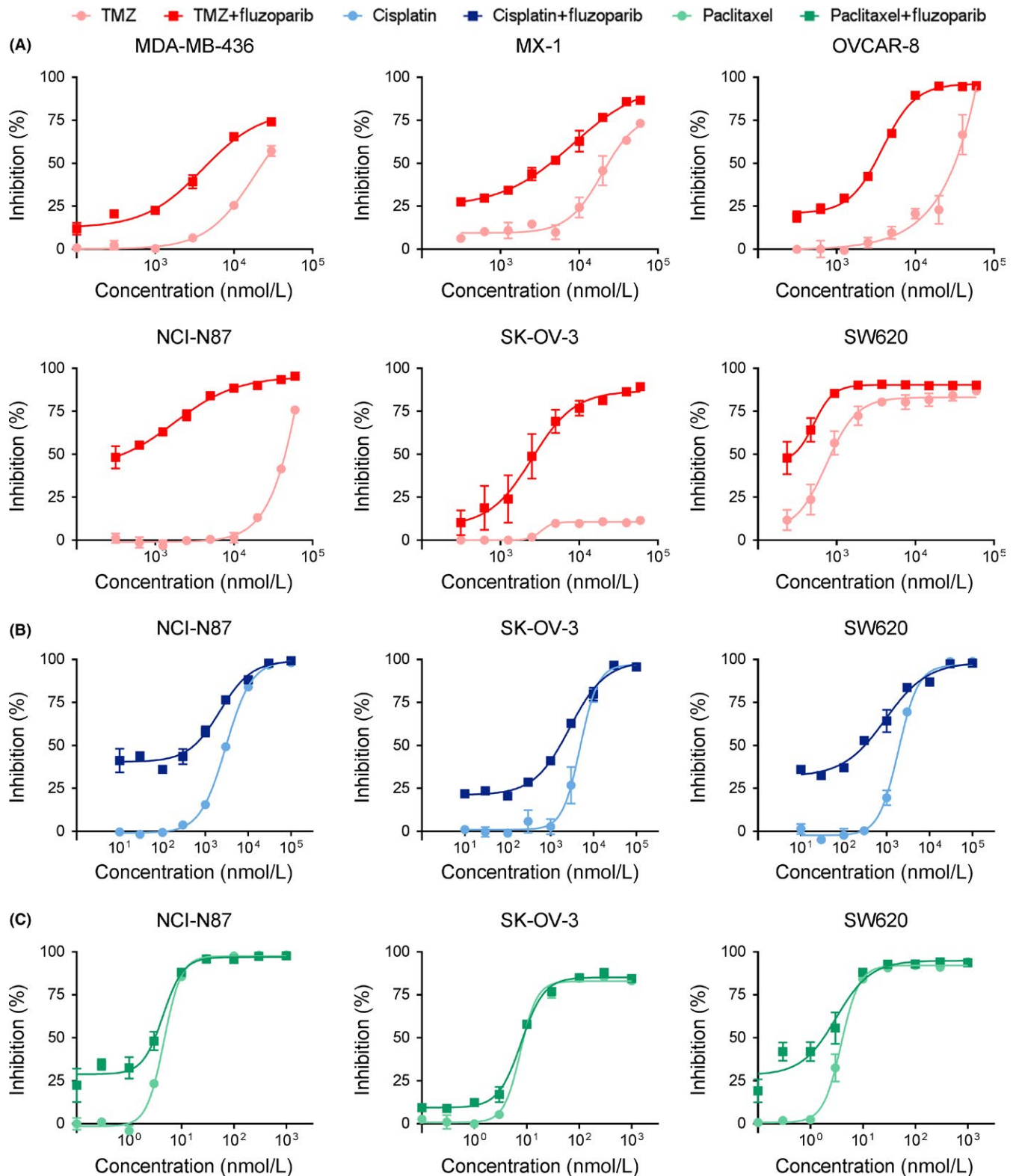


**FIGURE 3** Fluzoparib sensitizes cancer cells to cytotoxic drugs. Cells were treated with fluzoparib combined with temozolomide (TMZ) (A), cisplatin (B), or paclitaxel (C) for 120 hours, and cell proliferation was measured using sulforhodamine B assays. Data shown represent mean  $\pm$  SD of 3 independent experiments

treatment caused significant loss of body weight (Figure 6A). Fluzoparib is more potent than olaparib in the MDA-MB-436 xenograft model.

Given the profound activity of fluzoparib in sensitizing TMZ-induced growth inhibition, the antitumor potential of fluzoparib in combination with TMZ was further investigated in vivo.

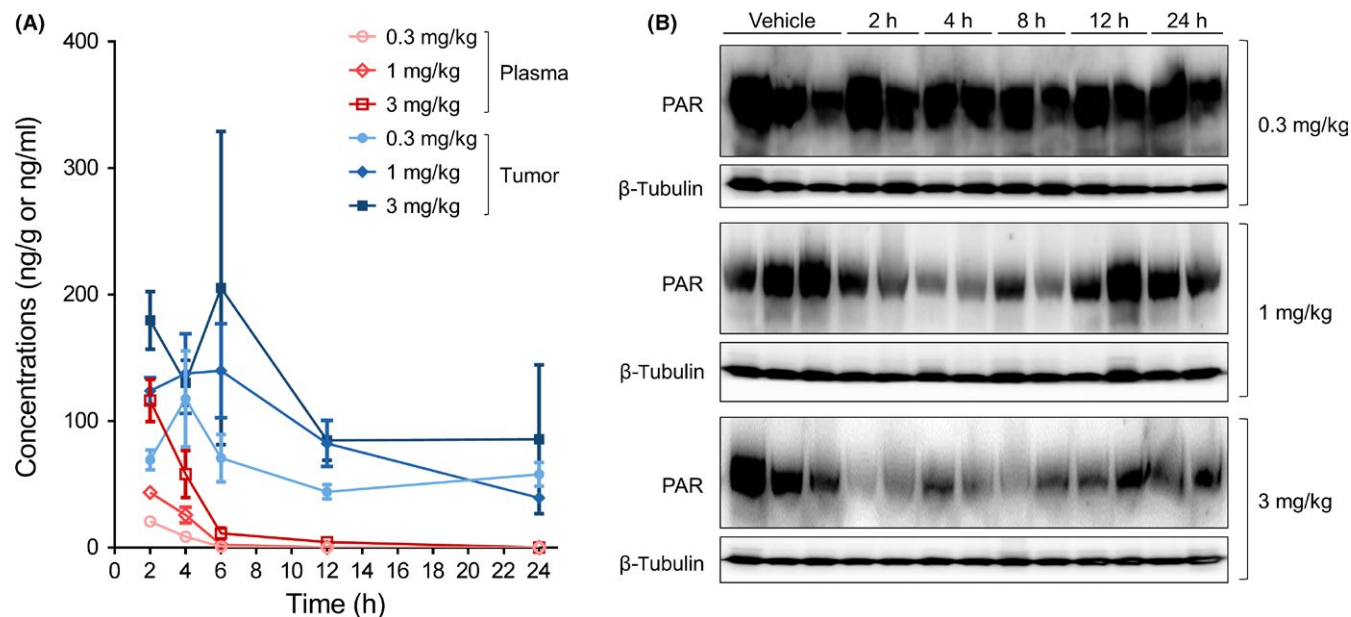


**FIGURE 4** Pharmacokinetic/pharmacodynamic characteristics of fluzoparib in an MDA-MB-436 xenograft model. Mice bearing MDA-MB-436 xenografts received a single dose (p.o.) of fluzoparib (0.3, 1, or 3 mg/kg) and were killed at the indicated times. A, Concentrations of fluzoparib in plasma and tumor were determined. B, Tumor extracts were analyzed by western blotting. PAR, polymer of ADP-ribose

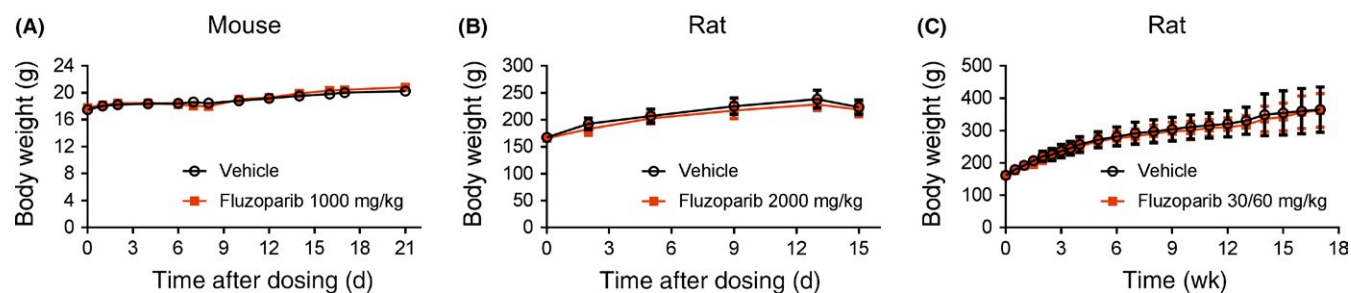


**FIGURE 5** Acute and chronic toxicity of fluzoparib. A, Female mice received fluzoparib at 1000 mg/kg. B, Female rats received fluzoparib at 2000 mg/kg. C, Female rats received fluzoparib at 30 mg/kg for the first 66 days, at 60 mg/kg for the next 24 days, and then were observed for another 28 days without treatment. Body weight was measured at the indicated days

In the MDA-MB-436 (*BRCA1*-deficient) xenograft model, fluzoparib (3 mg/kg) or TMZ (50 mg/kg) alone had no apparent inhibition on tumor growth, but were extremely effective when combined together (Figure 6B). Fluzoparib sensitized TMZ in a dose-dependent manner with inhibition rates of 66, 99, and 153% (day 21) at 0.3, 1, and 3 mg/kg, respectively. Partial tumor regression was achieved in 4/6 and 6/6 mice (day 21) by 1 and 3 mg/kg of fluzoparib combined with TMZ, respectively. Olaparib also enhanced the efficacy of TMZ, leading to an inhibition rate of 142% (day 21) and causing partial tumor regression in 5/6 mice (day 21) at the dose of 3 mg/kg. Due to the toxicity caused by TMZ, drugs were given from day 0 to day 4. After drug withdrawal, tumor recurrence was observed in all groups, but could be inhibited again through repeated treatment (day 53 to day 57).

Better results were obtained in the MX-1 (*BRCA1*-deficient, *BRCA2*-mutated) xenograft model (Figure 6C). When combined with TMZ, fluzoparib showed profound antitumor activity with inhibition rates of 82%, 95%, and 121% (day 8) at 1, 3, and 10 mg/kg,

respectively, and partial tumor regression in 5/6 mice was observed at 10 mg/kg. Olaparib also enhanced the antitumor activity of TMZ, but the extent of tumor shrinkage was not as remarkable as that of fluzoparib at the same dosage. Olaparib caused inhibition rates of 61%, 70%, and 90% (day 8) at 1, 3, and 10 mg/kg, respectively, and no tumor regression was observed. To exclude the possibility of experimental error, we repeated the experiment in the MX-1 model (Figure 6D). Consistently, fluzoparib at 3 mg/kg elicited more potent antitumor activity (inhibition rate: 85%, day 8) compared with olaparib at 3 mg/kg (inhibition rate: 75%, day 8) and similar antitumor activity compared with olaparib at 10 mg/kg (inhibition rate: 82%, day 8).

Loss of body weight was observed after treatment with TMZ alone or in combination with PARP inhibitors. No severe toxicity was observed after treatment with fluzoparib alone (Figure 6).

Taken together, these data reveal the significant antitumor efficacy of fluzoparib.



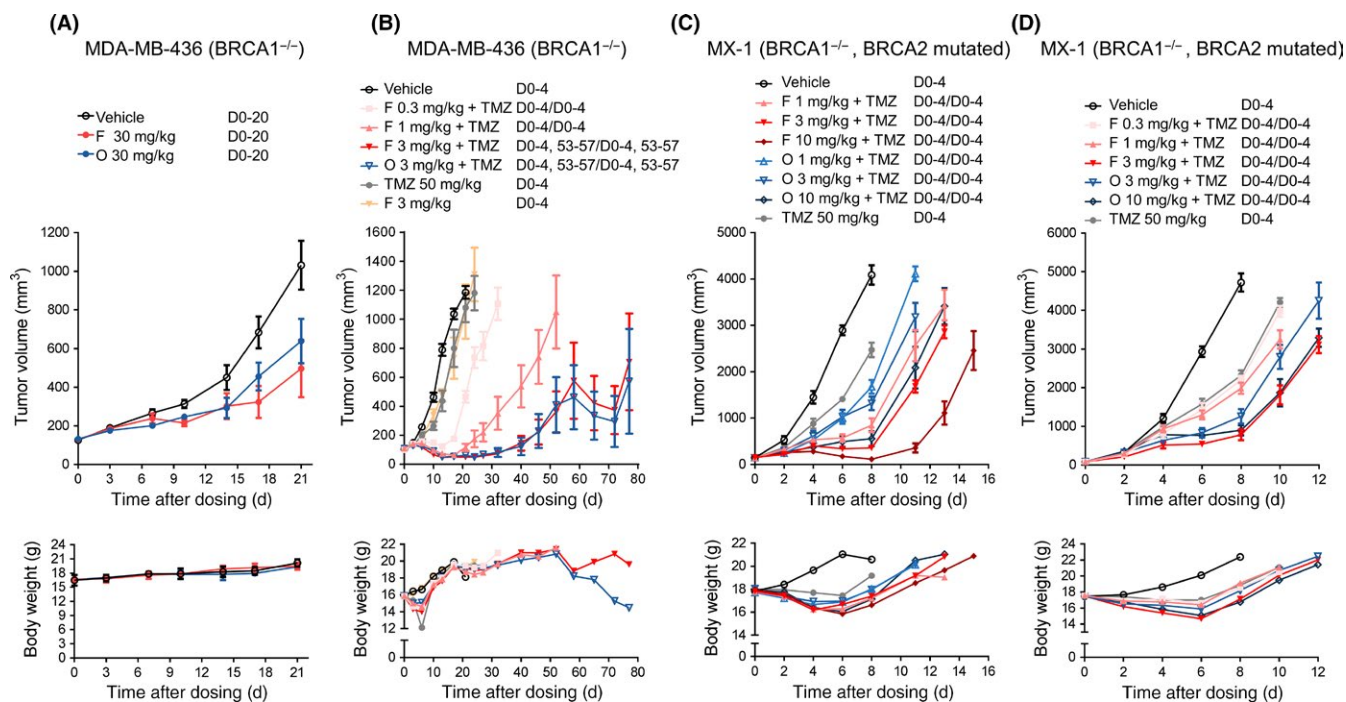


**FIGURE 6** Antitumor activity of fluzoparib in cell line-derived xenograft models. Nude mice bearing MDA-MB-436 (A,B) and MX-1 (C,D) xenografts were randomized into control ( $n = 10-12$ ) or treatment ( $n = 6$ ) groups. Control group was given vehicle and treatment groups were orally given fluzoparib (F), olaparib (O), and temozolomide (TMZ) (50 mg/kg) alone or in combination. Top panels, dosing schedule; bottom panels, tumor volume and body weight. Error bars represent mean  $\pm$  SEM. D, day

### 3.8 | In vivo antitumor activity of fluzoparib in cancer PDX models

Because fluzoparib could also potentiate cytotoxic drugs in *BRCA* WT cancer cells (Figure 3), we further explored combination regimens of fluzoparib in *BRCA* WT models in vivo. A PDX model in nude mice established with gastric cancer tissue from a patient (STO#069, *BRCA* WT) was used in this study. As the combination of PARP inhibitor with TMZ caused apparent toxicity (Figure 6), we explored the efficacy and toxicity of fluzoparib combined with other drugs. In consideration of the weak synergy of PARP inhibitors combined with cisplatin or paclitaxel in vitro and the unsatisfactory results in clinical trials,<sup>13,16</sup> we here explored whether apatinib, an inhibitor of vascular endothelial growth factor receptor-2, could enhance the antitumor activity of fluzoparib or conventional combinations (fluzoparib + cisplatin; fluzoparib + paclitaxel). As shown in Figure 7, 2-drug combinations of fluzoparib with cisplatin, paclitaxel, or apatinib caused growth inhibition with rates of 61.4%, 55.3%, and 72.8% (day 21), respectively; 3-drug combinations of fluzoparib, cisplatin, and apatinib or of fluzoparib, paclitaxel, and apatinib caused growth inhibition with rates of 84.9% and 75.6% (day 21), respectively. The 2-drug combination of fluzoparib with cisplatin and 3-drug combination of fluzoparib, cisplatin, and apatinib caused loss of body weight, whereas no apparent toxicity was observed in other combinations (Figure 7). Given the significant antitumor activity and tolerable profile of the 2-drug combination of fluzoparib with

apatinib and 3-drug combination of fluzoparib, apatinib, and paclitaxel, phase I studies to evaluate the tolerability and efficacy of these 2 combinations have been initiated (NCT03075462 and NCT03026881).

## 4 | DISCUSSION

Fluzoparib is a novel PARP inhibitor undergoing clinical trials. Here, we present the first report of the preclinical pharmacological results of fluzoparib and showed that fluzoparib showed potent anticancer activities in vitro and good pharmacokinetic properties, favorable toxicity profile, robust anti-tumor activity in vivo.

A remarkable characteristic of fluzoparib was its superior performance to olaparib in multiple human tumor xenografts models in vivo. In MDA-MB-436 xenografts model, fluzoparib was superior to olaparib when given alone or in combination with TMZ. Moreover, 2 independent MX-1 xenograft experiments further confirmed the advantage of fluzoparib. The remarkable antitumor activity of fluzoparib could result from 2 aspects, as discussed below.

First, fluzoparib displayed potent anticancer activities in vitro. Fluzoparib bound to PARP1 with the same binding mode as olaparib and showed potent inhibitory activity against PARP1 enzyme. Moreover, fluzoparib increased the formation of Rad51 foci and the level of  $\gamma$ H2AX, indicating DSBs were induced. These effects led to apparent G<sub>2</sub>/M arrest, apoptosis, and selective cell killing in *BRCA*-deficient cells. Furthermore, fluzoparib also effectively sensitized

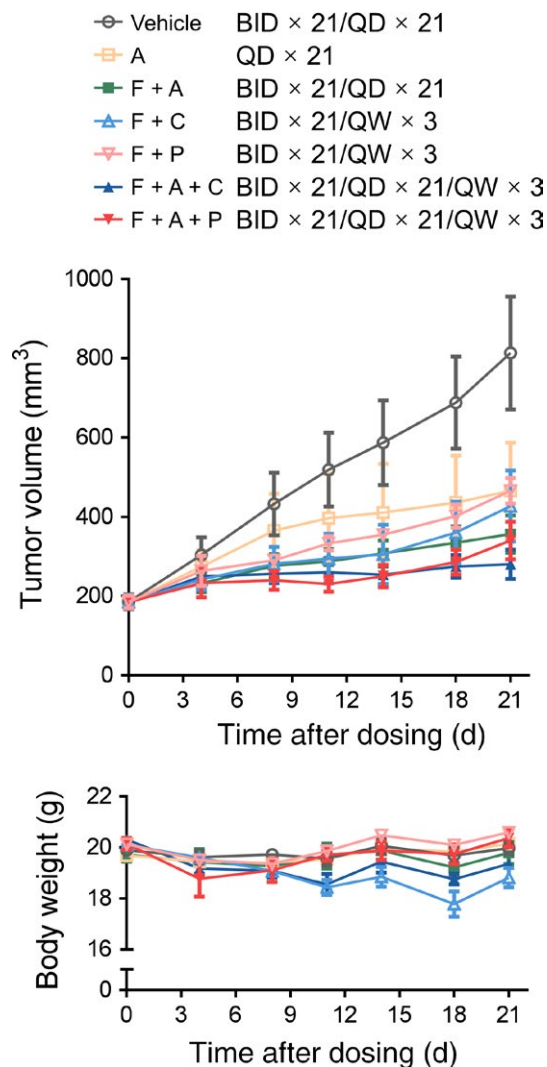


**FIGURE 7** Antitumor activity of fluzoparib in patient-derived xenograft models. Nude mice bearing xenografts derived from gastric tumor of a patient were randomized into control ( $n = 6$ ) or treatment ( $n = 6$ ) groups. Control group was given vehicle and treatment groups were given fluzoparib (F, 30 mg/kg, p.o.), apatinib (A, 50 mg/kg, p.o.), cisplatin (C, 5 mg/kg, i.p.), and paclitaxel (P, 15 mg/kg, i.p.) alone or in combination. Top panel, dosing schedule; bottom panel, tumor volume and body weight. Error bars represent mean  $\pm$  SEM

cancer cells to cytotoxic drugs. The *in vitro* anticancer activities of fluzoparib were comparable to that of olaparib, which provided a basis for the significant antitumor activity *in vivo*.

Second, fluzoparib had favorable pharmacokinetic/pharmacodynamic properties. In the MDA-MB-436 xenografts model, fluzoparib was rapidly absorbed and showed much higher exposure in tumor than plasma. Moreover, the concentrations of fluzoparib in tumor remained at high levels even at 24 hours after treatment. It is noteworthy that the calculated oil-water partition coefficients (log-P) of fluzoparib (4.2) was higher than that of olaparib (3.0), which indicated that the lipid solubility of fluzoparib was better than olaparib. The better lipid solubility of fluzoparib might make it easier to enter

xenografts. Olaparib has been shown to be excluded from the central nervous systems under normal conditions but reliably penetrated recurrent glioblastoma at therapeutic levels.<sup>7</sup> It was assumable that fluzoparib might be easier to cross the blood-brain barrier and have a potential advantage in the treatment of brain tumor. More importantly, the exposure and bioavailability of fluzoparib in female rats were both higher than those of olaparib.<sup>20</sup> All these data supported that fluzoparib was a drug with favorable pharmacokinetic/pharmacodynamic properties. Another significant characteristic of fluzoparib was its favorable toxicity profile. It has been reported that hematologic toxicities, including neutropenia, thrombocytopenia, and anemia are major adverse effects of PARP inhibitors and greatly limit their clinical application.<sup>21</sup> In an acute toxicity study of olaparib, a single oral dose at 300 mg/kg in female rats led to animal death on day 2 and produced abnormal clinical signs, such as salivation, lachrymation, hypothermia, hunched posture, and palpebral closure.<sup>20</sup> In this study, we raised the dose of fluzoparib to 1000 mg/kg in female mice and 2000 mg/kg in female rats; even so, no mortality or adverse signs were found. In a chronic toxicity study of olaparib, continuous oral dosing at 40 mg/kg for 28 days in female rats caused weight-easing, hematologic toxicities (changes in white cell populations, red blood cell parameters, and the precursor hematopoietic cells in the bone marrow) and histopathological changes (bone marrow, spleen, liver, and thymus).<sup>20</sup> In this study, fluzoparib was given orally for a longer time (30 mg/kg for the first 66 days and 60 mg/kg for the next 24 days) in female mice. Remarkably, no abnormal changes in clinical signs or body weights were observed in this process. Thus, fluzoparib was a drug with greatly improved safety profiles compared to olaparib.

A phase I study evaluating the food-effect of 1-dose fluzoparib in healthy subjects has been completed (NCT03062982). Fluzoparib is currently being investigated in a phase II study to evaluate its efficacy and safety in *BRCA1/2*-mutant relapsed ovarian cancer (NCT03509636). Preliminary results showed that fluzoparib had favorable pharmacokinetic properties and remarkable antitumor activity. These results confirm the findings in preclinical research and make fluzoparib an attractive PARP inhibitor.

As PARP inhibitors are a class of anticancer agents that target defects in DNA repair, the clinical application of PARP inhibitors as monotherapy is restricted mainly to *BRCA*-mutated, platinum-sensitive ovarian and breast cancers. To expand the indication of PARP inhibitors, we explored several combination regimens and found that the 2-drug combination of fluzoparib with apatinib and 3-drug combination of fluzoparib, apatinib, and paclitaxel showed improved antitumor effects without increased toxicity in a *BRCA* WT gastric cancer PDX model. Apatinib is a vascular endothelial growth factor receptor-2 inhibitor approved by the China Food and Drug Administration for the treatment of late-stage gastric cancer.<sup>22</sup> It is suggested that anti-angiogenic drugs act by blocking angiogenesis and, as a consequence, inducing hypoxia.<sup>23</sup> Chronic hypoxia can decrease the synthesis of *BRCA1*<sup>24</sup> and *RAD51*,<sup>25</sup> and thus decrease HR in cancer cells.<sup>25</sup> Several studies report that anti-angiogenic drugs can potentiate PARP inhibitors.<sup>26</sup> Here, we show that fluzoparib combined with apatinib shows robust antitumor activity.

Based on these data, a phase I study to evaluate the tolerability and efficacy of fluzoparib in combination with apatinib in recurrent ovarian cancer or triple negative breast cancer has been initiated (NCT03075462). In addition, we find that the 3-drug combination of fluzoparib, apatinib, and paclitaxel showed improved antitumor effects without increased toxicity. This is the first report to suggest that the combination of a PARP inhibitor with an anti-angiogenic drug can potentiate the efficacy of cytotoxic agents. Based on this finding, a phase I study to evaluate the tolerability and efficacy of fluzoparib in combination with apatinib and paclitaxel in recurrent and metastatic gastric cancer that progresses following first-line therapy has been initiated (NCT03026881).

Together, our study showed that fluzoparib, characterized as a novel PARP inhibitor, had potent antitumor activity in preclinical models. Fluzoparib potently inhibited PARP1 enzyme activity, induced persistent DSBs, G<sub>2</sub>/M arrest, and apoptosis in HR-deficient cells, selectively inhibited the proliferation of HR-deficient cells, and sensitized both HR-deficient and HR-proficient cells to cytotoxic drugs. Fluzoparib showed good pharmacokinetic properties, favorable toxicity profile, and robust in vivo antitumor activity. In particular, fluzoparib in combination with apatinib, or in combination with paclitaxel plus apatinib, showed remarkable antitumor effects without increased toxicity. All these features supported its undergoing clinical trials.

## ACKNOWLEDGMENTS

This work was supported by grants from the National Natural Science Foundation of China (No. 81502636), the Shanghai Science and Technology Committee (No. 14DZ2294100), and the Yunnan Provincial Science and Technology Department (No. 2017ZF010). We thank Professor Jianguo Sun (China Pharmaceutical University) for helping in the pharmacokinetic study and Jing Xing (Shanghai Institute of Materia Medica) for helping in the molecular docking.

## CONFLICTS OF INTEREST

Changyong Yang and Jiahua Jiang are employees of Jiangsu Hengrui Medicine Co Ltd. No potential conflicts of interest were disclosed by the other authors.

## ORCID

Liguang Lou  <https://orcid.org/0000-0001-7396-7122>

## REFERENCES

- Rouleau M, Patel A, Hendzel MJ, Kaufmann SH, Poirier GG. PARP inhibition: PARP1 and beyond. *Nat Rev Cancer*. 2010;10:293-301.
- Muthurajan UM, Hepler MR, Hieb AR, et al. Automodification switches PARP-1 function from chromatin architectural protein to histone chaperone. *Proc Natl Acad Sci USA*. 2014;111:12752-12757.
- Schreiber V, Dantzer F, Ame JC, de Murcia G. Poly(ADP-ribose): novel functions for an old molecule. *Nat Rev Mol Cell Biol*. 2006;7:517-528.
- Bryant HE, Schultz N, Thomas HD, et al. Specific killing of BRCA2-deficient tumours with inhibitors of poly(ADP-ribose) polymerase. *Nature*. 2005;434:913-917.
- Farmer H, McCabe N, Lord CJ, et al. Targeting the DNA repair defect in BRCA mutant cells as a therapeutic strategy. *Nature*. 2005;434:917-921.
- Brown JS, Kaye SB, Yap TA. PARP inhibitors: the race is on. *Br J Cancer*. 2016;114:713-715.
- Zhou JX, Feng LJ, Zhang X. Risk of severe hematologic toxicities in cancer patients treated with PARP inhibitors: a meta-analysis of randomized controlled trials. *Drug Des Devel Ther*. 2017;11:3009-3017.
- Mirza MR, Monk BJ, Herrstedt J, et al. Niraparib maintenance therapy in platinum-sensitive, recurrent ovarian cancer. *N Engl J Med*. 2016;375:2154-2164.
- Coleman RL, Oza AM, Lorusso D, et al. Rucaparib maintenance treatment for recurrent ovarian carcinoma after response to platinum therapy (ARIEL3): a randomised, double-blind, placebo-controlled, phase 3 trial. *Lancet*. 2017;390:1949-1961.
- Fong PC, Boss DS, Yap TA, et al. Inhibition of poly(ADP-ribose) polymerase in tumors from BRCA mutation carriers. *N Engl J Med*. 2009;361:123-134.
- Pujade-Lauraine E, Ledermann JA, Selle F, et al. Olaparib tablets as maintenance therapy in patients with platinum-sensitive, relapsed ovarian cancer and a BRCA1/2 mutation (SOLO2/ENGOT-Ov21): a double-blind, randomised, placebo-controlled, phase 3 trial. *Lancet Oncol*. 2017;18:1274-1284.
- Bundred N, Gardovskis J, Jaskiewicz J, et al. Evaluation of the pharmacodynamics and pharmacokinetics of the PARP inhibitor olaparib: a phase I multicentre trial in patients scheduled for elective breast cancer surgery. *Invest New Drugs*. 2013;31:949-958.
- Drean A, Lord CJ, Ashworth A. PARP inhibitor combination therapy. *Crit Rev Oncol Hematol*. 2016;108:73-85.
- Middleton MR, Friedlander P, Hamid O, et al. Randomized phase II study evaluating veliparib (ABT-888) with temozolomide in patients with metastatic melanoma. *Ann Oncol*. 2015;26:2173-2179.
- Bang YJ, Xu RH, Chin K, et al. Olaparib in combination with paclitaxel in patients with advanced gastric cancer who have progressed following first-line therapy (GOLD): a double-blind, randomised, placebo-controlled, phase 3 trial. *Lancet Oncol*. 2017;18:1637-1651.
- Dawicki-McKenna JM, Langelier MF, DeNizio JE, et al. PARP-1 activation requires local unfolding of an autoinhibitory domain. *Mol Cell*. 2015;60:755-768.
- Wang L, Xu Y, Fu L, Li Y, Lou L. (5R)-5-hydroxytryptolide (LLDT-8), a novel immunosuppressant in clinical trials, exhibits potent antitumor activity via transcription inhibition. *Cancer Lett*. 2012;324:75-82.
- Dziadkowiec KN, Gasiorowska E, Nowak-Markwitz E, Jankowska A. PARP inhibitors: review of mechanisms of action and BRCA1/2 mutation targeting. *Prz Menopauzalny*. 2016;15:215-219.
- O'Connor MJ. Targeting the DNA damage response in cancer. *Mol Cell*. 2015;60:547-560.
- CHMP assessment report-Lynparza. *European Medicines Agency*, 2014.
- Chalmers AJ, Jackson A, Swaisland H, et al. Results of stage 1 of the oparatic trial: a phase I study of olaparib in combination with temozolomide in patients with relapsed glioblastoma. *J Clin Oncol*. 2014;32:2025.
- Brower V. Apatinib in treatment of refractory gastric cancer. *Lancet Oncol*. 2016;17:e137.
- Al-Abd AM, Alamoudi AJ, Abdel-Naim AB, Neamatallah TA, Ashour OM. Anti-angiogenic agents for the treatment of solid tumors: potential pathways, therapy and current strategies – a review. *J Adv Res*. 2017;8:591-605.

24. Bindra RS, Gibson SL, Meng A, et al. Hypoxia-induced down-regulation of BRCA1 expression by E2Fs. *Cancer Res.* 2005;65:11597-11604.
25. Bindra RS, Schaffer PJ, Meng A, et al. Down-regulation of Rad51 and decreased homologous recombination in hypoxic cancer cells. *Mol Cell Biol.* 2004;24:8504-8518.
26. Gadducci A, Guerrieri ME. PARP inhibitors alone and in combination with other biological agents in homologous recombination deficient epithelial ovarian cancer: from the basic research to the clinic. *Crit Rev Oncol Hematol.* 2017;114:153-165.

**How to cite this article:** Wang L, Yang C, Xie C, et al. Pharmacologic characterization of fluzoparib, a novel poly(ADP-ribose) polymerase inhibitor undergoing clinical trials. *Cancer Sci.* 2019;110:1064–1075. <https://doi.org/10.1111/cas.13947>